

Flexible Polymer-on-Polymer Architecture for Piezo/Pyroelectric Energy Harvesting

Pejman Talemi,^{†,‡,§} Marine Delaigue,[†] Peter Murphy,[†] and Manrico Fabretto^{*,†}

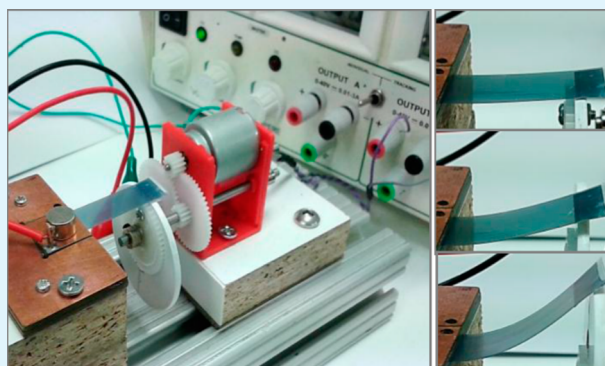
[†]Thin Film Coatings Group, Mawson Institute, University of South Australia, Mawson Lakes, 5095 South Australia, Australia

[‡]Department of Chemistry, University of Adelaide, Adelaide, 5001 South Australia, Australia

Supporting Information

ABSTRACT: An all polymer piezo/pyroelectric device was fabricated using β phase poly(vinylidene fluoride) (PVDF) as the active material and vapor phase polymerized (VPP) poly(3,4-ethylenedioxythiophene) (PEDOT) as the flexible electrode overlay material. Inherent problems usually associated with coating polymeric electrodes onto the low surface energy PVDF were overcome by air plasma treating the film in conjunction with utilizing the VPP technique to simultaneously synthesize and in situ deposit the PEDOT electrode. Strain measurements up to the breaking-strain of PVDF (approximately 35%) indicated that the change in R/R_0 was significantly smaller for the PEDOT based electrodes compared to the platinum electrode. Plasma treatment of the PVDF film increased the level of surface oxygenated carbon species that contributed to increased surface energy, as confirmed by contact angle measurement. The enhanced adhesion between the two polymers layers contributed to a significant increase in the measured piezoelectric output voltage from 0.2 to 0.5 V for the same strain conditions. Pyroelectric voltage outputs were obtained by placing the film onto and off of a hotplate, for temperatures up to 50 °C above ambient. Finally, as a proof of concept, a simple energy harvesting device (plastic tube with slots for mounting multiple piezo/pyro films) was fabricated. The device was able to generate a usable level of peak output current ($>3.5 \mu\text{A}$) from human inhalation and exhalation “waste energy”.

KEYWORDS: piezoelectric, pyroelectric, flexible electrodes, vapor phase polymerization, PEDOT, PVDF



INTRODUCTION

The growing society driven demand for accessible and environmentally sustainable energy generation represents a significant challenge for the material scientist tasked with delivering alternate energy sources. Large-scale examples that convert mechanical actuation into electrical energy include systems such as wind, river or tidal flow generators.^{1,2} At the other extreme, small-scale harvesters can be used to scavenge “waste energy” from mechanical vibrations associated with industrial, environmental or human activity.^{3,4} For small-scale applications, especially ones involving human activity, there is a push to incorporate rechargeable wearable electronics onto the end user. This has placed a premium on conformable and flexible polymeric materials that have the ability to convert mechanical energy into electrical energy.

Piezoelectric devices offer an option for harvesting “waste energy” in the form of wind,⁵ acoustic,⁶ vibrations in buildings and cars,⁷ and human movement.^{8,9} Harvesting energy from autonomic body movement (e.g., heart beats and respiration) or human activity (e.g., jogging) provides a means for developing self-charging biomedical devices or wearable electronics. Some of the recent work in this area has focused on exploring novel materials such as graphene oxide films⁶ and

hybrid structures based on ZnO nanowire.⁸ However, polymeric piezoelectric materials such as poly(vinylidene fluoride) (PVDF) are readily available, flexible, and are able to provide a high level of piezoelectric conversion (i.e., comparable or higher than the aforementioned novel materials). Additionally, the polymer is chemically stable, has good weathering characteristics and offers the level of flexibility required for wearable electronic applications.¹⁰ Untreated PVDF exists in either; α , β , or γ crystalline phases, but mechanically stretching and poling the polymer produces the β phase which is the necessary condition for producing piezoelectricity. Additionally, PVDF exhibits pyroelectric properties that enable the polymer to convert temperature changes into electricity.^{11,12} This makes the polymer an ideal candidate for generating electrical energy by means of converting both mechanical and thermal processes. In fact, piezo/pyroelectric energy generation using PVDF has already been demonstrated in human-activities such as breathing, walking, jogging, running, etc. by incorporating the material

Received: December 17, 2014

Accepted: March 25, 2015

Published: March 25, 2015



into the soles of shoes and backpacks, or by capturing the respiration process.^{9,13,14} To extract the generated charge, PVDF has traditionally been coated with thin metallic electrodes, which largely negates the inherent flexible nature of the material. Complementary to PVDF, inherently conducting polymers (ICPs) offer both flexibility and the ability to transport charge. These polymers are gradually finding their way into the next generation of electronic devices due, in part, to their high electrical conductivity,¹⁵ optical transparency,^{15,16} electrocatalytic performance^{17,18} and printing processability. This has resulted in ICPs being used for applications such as organic solar cells,^{19,20} fuel cells,^{17,18} electrochromic devices²¹ and OLEDs.²² The possibility of printing^{23,24} and patterning²⁵ these polymers combined with their electroactive properties makes them suitable for many organic electronic applications.²⁶ The main advantage of using polymeric electrodes instead of metallic electrodes with respect to piezo/pyroelectric generation is, however, their innate flexibility.²⁷ The next generation of electronic devices employing wearable electronics and implantable devices will require conductive, flexible and stretchable conductors. For this reason, many researchers in recent years have focused on developing flexible conductors based on conducting polymers.^{20,27–30} Much of the drive stems from the desire of wanting to print flexible electrodes/conductors (and other active layers) in an effort to produce cheap reel-to-reel flexible solar energy harvesting devices.^{20,27} Although developing flexible solar cells has some practical advantages, printability rather than flexibility is the main driver/requirement for cheap solar energy harvesting. The printability and flexibility however also makes them good candidates as electrode materials for piezo/pyroelectric devices.

The poor adhesion and (relative) brittleness of metal electrodes on the hydrophobic PVDF have limited their application and some devices have suffered mechanical damage as a result of high elongation/deformation forces.^{11,31} To overcome this problem, some researchers have attempted to use conductive polymers as an alternate electrode material in piezoelectric devices.^{11,31–33} One of the most promising commercially available conductive polymers is poly(3,4-ethylenedioxythiophene)/poly(4-styrenesulfonate) (PEDOT/PSS). The polymer is typically supplied as an aqueous dispersion, which inherently makes coating the hydrophobic PVDF problematic. As a result, the coating process suffers from dewetting, which adversely affects film formation, adhesion and conductivity. One of the advantages of vacuum vapor phase polymerized (VPP) PEDOT is that it is able to be synthesized in situ onto donor substrates. This process should overcome the issues associated with applying aqueous dispersions onto hydrophobic surfaces. In this paper, the preparation and coating process onto the PVDF was examined with a view to obtaining a uniform PEDOT electrode coating and then testing the electromechanical properties of the coating. Subsequently, the all polymer composite material was tested for its piezo/pyroelectric energy harvesting response. Finally, the material was incorporated into a device for human-motion “waste energy” harvesting and simultaneously recorded piezo/pyroelectric output.

EXPERIMENTAL SECTION

All PEDOT coatings were deposited using vacuum vapor phase polymerization using a previously described oxidant recipe.^{15,16,34} The 3,4-ethylenedioxythiophene (EDOT) monomer and Fe(III) Tosylate

oxidant (CB-40) solution were obtained from Clevios. The triblock copolymer poly(ethylene glycol–propylene glycol–ethylene glycol) (PEG–PPG–PEG) and ethanol were purchased from Sigma. Prior to coating, the stretched and poled β phase KF Piezo PVDF (Kureha Corporation, Japan, 110 μm and piezoelectric constant d_{31} of 25 pC/N) film was air plasma treated (Diener, NANO, 40 kHz, 0–300 W_{max}) from 0 to 10 min to modify the chemistry at the surface and improve the adhesion and interaction between PEDOT and PVDF. To ensure the film temperature remained below the Curie temperature (165 °C) during low-temperature plasma treatment, a TinyTags thermistor data logger (100 Ohm NTC low thermal mass element) was mounted onto the PVDF film. The plasma treated PVDF films were coated with the oxidant solution on both sides by dip coating. Changing the speed of the dip coating process (0.1 to 1 mm/s) made it possible to control the thickness of the deposited oxidant layer and the resultant PEDOT films. The oxidant coated PVDF was placed into the VPP chamber and exposed to EDOT monomer vapor for 25 min. After the polymerization process, the samples were washed in an ethanol bath to remove the spent residual oxidant, leaving behind a PEDOT coated PVDF film. Platinum coatings of approximately 30 nm were deposited onto the PVDF films using an in-house physical vapor deposition (PVD) chamber running a Pt sputter target. PVDF films were coated using a single pass at 200 W in an argon gas environment running at a base pressure of 2×10^{-3} mbar.

Changes in the surface chemistry of the PVDF films were analyzed using X-ray photoelectron spectroscopy (XPS) using a SPECS SAGE XPS system. All the results presented here were obtained using Mg $K\alpha$ ($h\nu = 1253.6$ eV), operated at 10 kV and 10 mA (100W). The background pressure was 2.0×10^{-6} Pa. Pass energy of 100 eV and energy steps of 0.5 eV were used to obtain wide scan spectra, whereas 20 eV pass energy and energy steps of 0.1 eV were used for the high-resolution spectra of the C 1s and O 1s core line peaks. Spectra were analyzed using CASAXPS (Neil Fairley, UK). X-ray diffraction (XRD) was performed using a Scintag ARL X'Tra instrument using Cu $K\alpha$ radiation of wavelength 1.54 Å. Scans were conducted from 16 to 24° 2θ at 0.02° intervals at a rate of 0.08°/min. Atomic force microscopy (AFM) images and measurements (NTEGRA, NT-MDT) were performed in tapping mode, scan size $1 \times 1 \mu\text{m}$. To measure the relative change in the surface energy of the plasma treated PVDF, static (advancing) water contact angles were obtained using a Data-Physics OCA15 contact angle analyzer (DataPhysics Instruments GmbH, Filderstadt, Germany). The change in normalized sheet resistance R/R_0 versus strain were recorded on an Instron 5567 (± 30 kN static load cell) tensile tester in conjunction with an in-house clamping system connected to an autoranging multimeter. Piezoelectric outputs were measured by applying a bending force onto the 30 \times 10 mm PVDF strip using an in-house built mechanical rotating cam actuator (see Figure S5 of the Supporting Information). Pyroelectric outputs were obtained by placing the PVDF strip onto a hotplate set to different temperatures. Both the open circuit voltage and the power delivered into a 60 M Ω resistive load were measured. The piezo/pyroelectric output was measured using an in-house build device (plastic tube containing slots for mounting multiple PVDF strips in either parallel or series configuration) containing the PVDF film(s) in conjunction with human breathing (inhalation/exhalation).

RESULTS AND DISCUSSION

Substrate Preparation. The focus of this work was to coat the PVDF piezoelectric material with an electrode, which would not compromise its flexibility under strain conditions. Traditional electrode materials are typically metallic, and under repeated stretching/bending actuation, these electrodes may suffer microstructural damage, which leads to cracking (with an associated increase in electrode resistance) and may ultimately cause delamination from the piezoelectric substrate. This severely limits the efficiency of the device and its ability to extract charge during mechanical deformation. Compounding the problem of finding a suitable flexible electrode material, the

low surface energy of PVDF generally results in poor film adhesion as well. For this reason, researchers have used methods such as ion-assisted-reaction to improve the adhesion at the electrode/PVDF interface.^{11,31} To ensure that the temperature of the PVDF did not exceed 165 °C (Curie temperature), a thermistor sensor TinyTags data logger was mounted in situ onto the film during plasma treatment to monitor the temperature. A maximum temperature of 65 °C was recorded, which was well below the Curie temperature (Figure S1 of the Supporting Information). To overcome problems associated with flexibility, the conducting polymer PEDOT was chosen as the electrode material. In this study, an air plasma treatment was used to enhance the surface energy of the PVDF films by partially oxidizing the surface. A qualitative measure for adhesion was established by measuring static advancing contact angles for the PVDF samples using the sessile drop technique. Based on the sessile drop measurements, an air plasma treatment of up to 6 min resulted in progressively lower contact angles (i.e., a higher energy surface) whereas plasma treatments longer than this produced a slight increase from the lowest recorded contact angle, as shown in Figure 1. To understand the chemistry behind this observation,

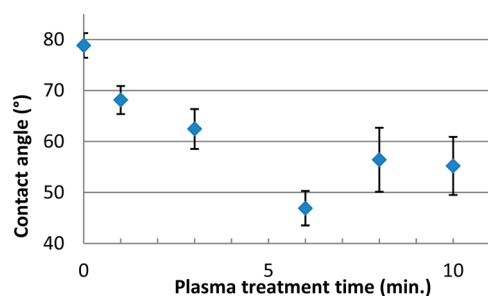


Figure 1. Changes in PVDF contact angle as a function of plasma treatment time. A qualitative measure of surface energy. (Note: a decrease in contact angle correlates with an increase in surface energy.)

XPS analysis was performed on the treated samples. XPS analysis of the plasma treated PVDF samples revealed that as plasma treatment time increased (up to 6 min) the surface elemental concentration of carbon and fluorine decreased while the concentration of oxygen increased (Table S1 of the Supporting Information). Continuing the plasma treatment beyond 6 min, however, had an opposite effect on the surface chemistry of PVDF films (i.e., increased fluorine and decreased oxygen). A more detailed analysis of the surface chemistry by deconvolution of the C 1s peak into its components (Figures S2 and S3 of the Supporting Information) indicated that the early stage plasma treatment resulted in the formation and rise of oxygenated functional groups and a concomitant decline in fluorinated carbon atoms. However, extending the plasma treatment beyond 6 min had the opposite effect on the concentration of oxygenated and fluorinated carbon atoms. Such changes in surface chemistry coupled with the decrease in contact angle are consistent with an increase in surface oxidation within the first 6 min of treatment. However, extending plasma treatment beyond this most likely leads to further oxidation of the oxygenated carbon atoms into gases like CO₂ and CO, or soluble fragmented polymer chains that are easily detached from the PVDF surface. Although it is also understood from the XPS results that the plasma treatment would compromise some of the β phase at the surface of the

PVDF film, the enhanced adhesion between the PVDF and PEDOT layers compensates for this loss, leading to increased charge output. XRD measurements (Figure S4 of the Supporting Information) performed on a 6 min plasma treated PVDF sample indicated a 28% decrease in the peak (maximum) located at 20.8° which is associated with the PVDF β phase.^{35,36} However, it must be stressed that the measurement had a “surface bias” and that the same loss would not be expected well below the surface of the film. As such, the overall loss in β phase for the film would, in reality, be significantly less than this. As explained in the following sections, piezoelectric devices based on 6 min plasma treated PVDF gave the best piezoelectric performance. Additionally, the various plasma treatments produced no discernible difference in the thickness of the subsequently VPP synthesized PEDOT, although it must be noted that this was difficult to quantify due to the soft nature of the underlying PVDF making it problematic to obtain accurate readings. If differences did exist, they did not impact on the results and are within the normal statistical errors associated with any individual measurement.

Flexible Electrodes. Vacuum vapor phase polymerization (VPP) was used for the deposition of thin layers of PEDOT onto the PVDF substrates. Previous studies have shown that VPP polymerization of PEDOT in the presence of a nonconducting polymer such as polyethylene glycol (PEG), polypropylene glycol (PPG), or a triblock copolymer based on both PEG and PPG dispersed within the oxidant solution results in the formation of an alloy of PEDOT and glycol.^{37,38} Besides the known beneficial effects that this additional polymer has on conductivity and film morphology,^{15,38} it also provides a plasticizing action that helps facilitate the slip-movement of adjacent polymer grains. Confirmation that PEDOT was synthesized and deposited on the PVDF film, using the VPP process, was straightforward, as the conducting polymer is dark blue in color. Additionally, AFM imaging (see Figure S6 of the Supporting Information) clearly showed the characteristic grain-like structure and using a multimeter confirmed electrical continuity across the PVDF strip. Establishing the exact film thickness in order to calculate the conductivity of the film was problematic due to the soft nature of the underlying PVDF. The same VPP conditions were used to synthesis PEDOT on glass substrates, and the polymerization time was altered to produce various film thicknesses. PEDOT films greater than approximately 80 nm recorded conductivity of the order of 2000 S/cm. Below this thickness, the conductivity fell to a low of approximately 300 S/cm at a film thickness of 20 nm. These results were used as a reference and are given in Figure S7 of the Supporting Information. The use of the glycol triblock copolymer PEG-PPG-PEG within the oxidant solution results in a PEDOT-glycol composite³⁹ during synthesis, and this should produce a conducting layer with increased flexibility and delayed crack formation under mechanical strain actuation. To confirm this, the electro-mechanical properties of the PEDOT film were tested by measuring the change in electrical resistance versus mechanical strain on an Instron tensile test instrument. To benchmark the result, a platinum coated PVDF sample was used as a performance comparison to that of the PEDOT coated samples. The dependence of resistance on strain can be theoretically modeled for a homogeneous conductor that has no internal structure and does not crack when stretched using the following relationship:²⁸

$$\frac{R}{R_0} = \frac{1 + \epsilon'}{(1 - \nu_s \epsilon')(1 - \nu_f \epsilon')} \quad (1)$$

where R/R_0 is the normalized resistance of the sample, ϵ' is the fractional strain and ν_s and ν_f are the Poisson ratio of the substrate and the film, respectively. Poisson ratio values of 0.35, 0.38 and 0.29 were used for PEDOT,²⁸ platinum⁴⁰ and PVDF (based on a technical report by Kureha), respectively. Figure 2

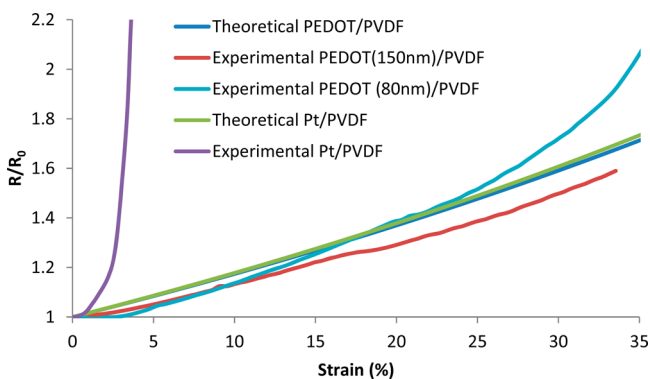


Figure 2. Theoretical and experimental plots of changes of normalized resistance as a function of applied strain for platinum and PEDOT.

shows the experimental and theoretical plots of normalized resistance versus strain for PVDF films coated with platinum or PEDOT. The normalized resistance (R/R_0) of the platinum coated PVDF increased rapidly once the %strain was increased beyond 0.5% and reached a maximum R/R_0 of 45 at a strain of 35% (note that the maximum $R/R_0 = 45$ is not shown in Figure 2). This was due to delamination and the formation of cracks, as a result of the poor adhesion between platinum and the PVDF substrate as well as the platinum being unable to elastically deform. Thus, one could argue that %strain values exceeding 0.5% would result in permanent damage of the platinum electrode with a subsequent decrease in the ability of the electrode to extract charge. However, for both the 80 and 150 nm PEDOT coated PVDF films, the R/R_0 follows the theoretical trend and, in fact, both experimental curves initially lie below the theoretical curve. This result is in agreement with previously reported studies^{28,41} where a similar PEDOT:PSS was used as the electrode material and indicates that the PEDOT resistance has decreased slightly in the strain direction due to the forced alignment of individual polymer grains. The forced alignment resulted in a lowering of the sheet resistance. In one of the previously reported studies, strains higher than 18% produced a rapid increase in normalized resistance due to the accumulation of cracks within the polymer film. This resulted in values well above the theoretically predicted resistance, yet in our case, such a transition (R/R_0 laying above the theoretical line) was only observed for the thinnest (80 nm) PEDOT film that was tested, and for values of %strain exceeding 25%. For the films in this study, the PEDOT grain size is of the order of 40–80 nm, which means that there exists only one or at most two effective grain layers in the thinnest film. The consequence of this is that the (conductivity) percolation threshold is lost at lower levels of %strain compared to the thicker film (150 nm), where up to four layers exist. Thus, the tensile stretching induces PEDOT grain alignment, which reduces the sheet resistance, but this is countered by an overall decreasing film thickness. Whichever of the two phenomena dominates dictates whether the R/R_0 lies either

above or below the theoretical R/R_0 line. For all other PEDOT film thicknesses greater than these values (Figure 2 shows 80 and 150 nm films), the experimental normalized resistance remained lower than the theoretical data over the 0 to 35% strain range. The upper strain limit of 35% was in fact due to the PVDF substrates not being able to withstand greater values without rupture (i.e., complete rupture at a stress of 300 MPa).

Piezoelectric Energy Harvesting. Placing strain across the PVDF induces the separation of charge, but effectively extracting this charge by coating the film with a metallic electrode layer is problematic. The metallic layer stiffens the PVDF film and additionally the electrode is prone to microcracking under repeated stress/strain actuation (refer to Figure 2). To test the performance of a nonmetallic electrode, a piezoelectric device consisting of a PVDF films coated with PEDOT on both sides was prepared. An in-house designed rig (Figure S5 of the Supporting Information) using a rotating cam (with variable frequency) exerted a bending force of ≈ 3 mN on the piezoelectric material while the output voltage was recorded. The difference between the peak-to-valley voltages were measured and averaged over a hundred cycles and reported as the voltage output. To study the frequency dependency (if any) of the piezoelectric material, samples with different plasma treatment times were strain tested in the frequency range 1–20 Hz. Figure 3a demonstrates that there

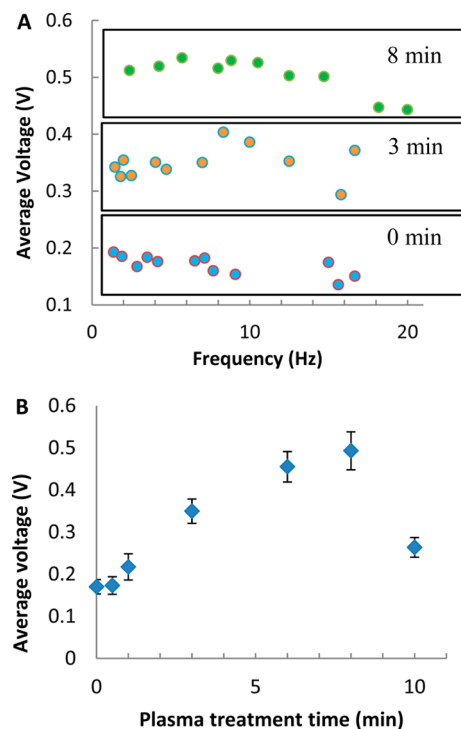


Figure 3. (A) Frequency dependency of piezoelectric PVDF samples with 3 different plasma treatment times, and (B) variation in piezoelectric output voltage as a function of plasma treatment time (note: at constant ambient temperature, $T_0 = 23$ °C).

was no discernible dependence between the frequency of the applied strain (at constant ambient conditions 23 °C) and the voltage output for the piezoelectric films up to 14 Hz. Beyond this frequency, mechanically induced flutter (i.e., the piezoelectric film was unable to intimately follow the cam profile) produced inconsistent voltage spikes and a slight drop in the average voltage was recorded. Importantly, there was a distinct

difference in the average voltage output for the PVDF samples produced with different plasma treatment times. PVDF samples treated for 0–10 min were prepared and their voltage output in the frequency range of 1–20 Hz was recorded and averaged. Figure 3b shows that samples with 6 and 8 min of plasma treatment exhibited the best piezoelectric performance. This result is in agreement with the surface chemistry analysis discussed previously and indicates that even though the topmost layer of the PVDF film under goes some form of chemical “damage” leading to a loss of the β phase, the better interaction (adhesion) between PEDOT and PVDF (induced by the plasma treatment) results in better charge transfer between the two polymers.

Pyroelectric Energy Harvesting. Using PVDF for energy harvesting by utilizing the polymer’s pyroelectric phenomenon has also been reported.^{11,12,42} Complementing the piezoelectric strategy for energy harvesting, similar PEDOT/PVDF/PEDOT films were fabricated to examine pyroelectric energy harvesting. Figure 4 shows the open circuit voltage time evolution as a

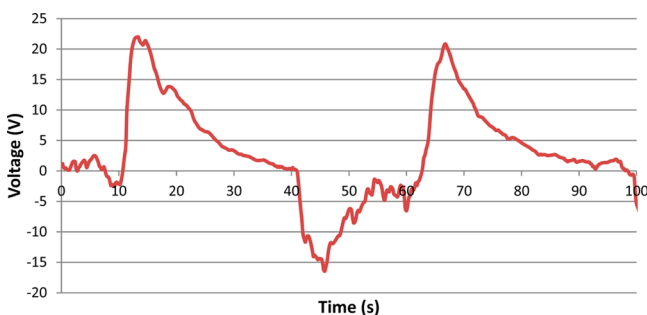


Figure 4. Time evolution open circuit voltage generated as a function of instantaneous temperature change (ambient temperature, $T_0 = 23$ °C) by placing the PVDF strip onto (positive voltage spike) a hotplate and then removing it from the hotplate (negative voltage spike).

result of placing the PVDF strip onto a hotplate (positive going voltage spike) and then removing the strip (negative going voltage spike). A sharp voltage output is initially produced when the PVDF strip is either placed onto or taken off of the hotplate, followed by an exponential decay as the temperature of the PVDF strip equilibrates. Figure 5a shows that the system was capable of converting temperature changes into significant open circuit output voltages simply by placing the strips onto a hotplate (note that the positive voltage has been arbitrarily assigned to temperature increases and the negative voltage to temperature decreases). Based on the results, a change of 16 °C

above ambient temperature (and then the removal of the sample) produced an open circuit output voltage of approximately 100 V. The maximum temperature used was ≈ 70 °C, which is well below the Curie temperature (i.e., ≈ 165 °C)⁴³ of the PVDF film and the onset of PEDOT polymer degradation (≈ 130 – 140 °C).⁴⁴ The PVDF device does, however, have a large internal resistance, so delivery of any usable power can only be maximized when the device is connected to high impedance loads or if the device’s active surface area is very large. A suitably large load resistor (i.e., 60 M Ω , which would be equivalent to the load of a low-power consumption IC circuit) was placed on the output of the device and the voltage across the resistor measured. The power output (i.e., $P = V^2/R$) of the device was calculated, and from Figure 5b, it can be seen that the PVDF based pyroelectric device was able to generate (harvest) more than 1 μ W of electrical power from a 52 °C temperature change. By selecting an applied load that matches the effective internal resistance of the PVDF device, the transferred power, for a given PVDF surface area, can be further increased. Alternatively, simply increasing the surface area of the PVDF film to as large as can be practically accommodated within the device will also lead to an increase in transferred power.

To combine the piezoelectric and pyroelectric phenomena in an effort to harvest “waste energy” from human activity (i.e., inhaling at ambient temperature ≈ 23 °C and exhaling ≈ 37 °C) a device consisting of multiple PEDOT-coated PVDF films positioned 90° apart with respect to each other were mounted within a plastic tube (as shown in Figure S8 of the Supporting Information). The generated output is shown in Figure 6. In this device, the PVDF films were able to bend and vibrate as a result of the air flow and this generated the piezoelectric effect. At the same time, due to the difference in temperature between inhalation of ambient air and the exhalation of air from the lungs, the resulting temperature oscillations also produced a pyroelectric effect. To evaluate the device, bursts of rapid panting were delivered into the tube and the maximum current flow into a short circuit load was measured (after passing through a full-wave bridge rectifier). A single PVDF film as well as multiple films (up to four) connected in series or parallel were investigated. The multiple films connected in series, rather than producing the addition of individual outputs, produced a rather poor response (results not show). This result is explained in terms of the outputs from each individual film not being a simple additive process but rather that the individual outputs were phase separated. For the most part, the phase separated output responses of each individual strip

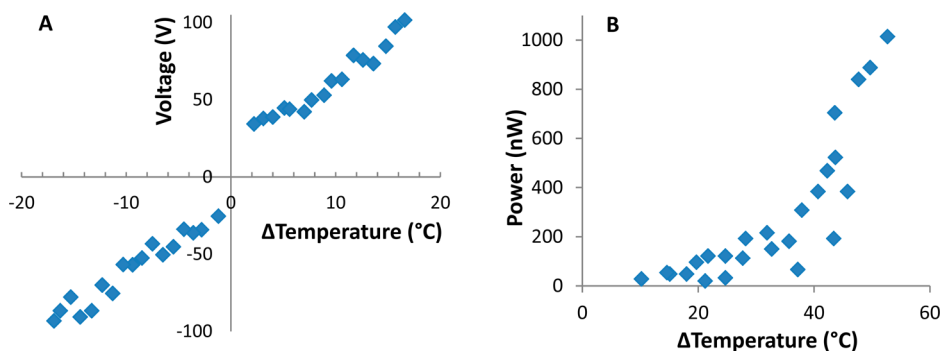


Figure 5. (a) Open circuit voltage generation as a function of temperature change (note: ambient temperature $T_0 = 23$ °C and 0% strain), and (b) generated power into a 60 M Ω load as a function of temperature change.

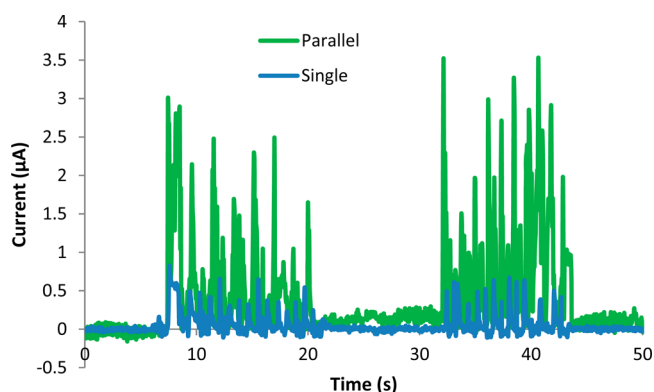


Figure 6. Current output of a single and multiple parallel PEDOT/PVDF/PEDOT energy harvesting films (note: current output due to variations in instantaneous temperature and %strain).

tended to produce an output well below the anticipated overall output. This is explained in terms of each PVDF strip fluttering/cooling/heating at different rates and randomly with respect to each other. A single PVDF film (Figure 6 blue trace) was connected and a maximum rectified current (full-wave rectified bridge using 1N5819 Schottky diodes) of approximately $0.75 \mu\text{A}$ was measured. It is appreciated that the use of ultralow leakage diodes (i.e., HSMS-280X series) would need to be incorporated into a charge collection circuit to maximize the stored charge. Connecting multiple elements in parallel resulted in an increase in the maximum current flow (Figure 6 green trace) with spikes of up to $3.5 \mu\text{A}$ recorded. Connecting the individual films in parallel effectively increased the active surface area without producing any detrimental effects as a result of the random nature by which each element fluttered/heated/cooled.

CONCLUSION

The flexible conducting polymer PEDOT was synthesized and deposited in situ using VPP and used as the electrode material in a PVDF based piezo/pyroelectric device. Strain measurements indicated that the change in R/R_0 all the way up to the breaking strain of PVDF ($\approx 35\%$) was significantly less than that for the platinum electrode, indicating PEDOT's suitability as a flexible electrode material. Applying an air plasma treatment on the PVDF film of (up to) 6 min produced oxygenated carbon functional groups on the surface of the film as measured using XPS and a concomitant reduction in the amount of fluorinated carbon atoms. The formation of a higher energy surface, as confirmed by contact angle measurements, provided for an increased adhesive interaction between the PEDOT coating and the PVDF film. The upshot of this increased interaction between the two polymers was an increase in the measured piezoelectric output voltage from 0.2 to 0.5 V under the same strain conditions produced by a mechanical cam actuator. Pyroelectric open circuit voltage outputs of up to 100 V and power outputs of up to $1 \mu\text{W}$ (into a $60 \text{ M}\Omega$ resistive load) were obtained by placing the film onto and off of a hotplate, for temperatures up to 50°C above ambient. As a proof of concept, a simple device was fabricated from a plastic tube with slots for mounting multiple PEDOT coated PVDF films that generated a usable level of current ($>3.5 \mu\text{A}$) from human inhalation and exhalation "waste energy". The design of a suitable low leakage electrical circuit could then be used to store the generated energy.

ASSOCIATED CONTENT

Supporting Information

Table S1: XPS elemental analysis for PVDF samples. Figures S1–S8: PVDF temperature during plasma treatment; XPS of plasma treated PVDF; at. % carbon species on PVDF; XRD measurements for untreated and treated PVDF; strain apparatus for PVDF films; AFM image of VPP PEDOT; VPP conductivity versus film thickness; Pyro tube. This material is available free of charge via the Internet at <http://pubs.acs.org>.

AUTHOR INFORMATION

Corresponding Author

*M. Fabretto. E-mail: Rick.fabretto@unisa.edu.au.

Present Address

[§]School of Chemical Engineering, University of Adelaide, Adelaide, South Australia 5005, Australia

Notes

The authors declare no competing financial interest.

REFERENCES

- (1) Lu, X.; McElroy, M. B.; Kiviluoma, J. Global Potential for Wind-Generated Electricity. *Proc. Natl. Acad. Sci. U. S. A.* **2009**, *106*, 10933–10938.
- (2) Scraggs, J.; Jacob, P. Harvesting Ocean Wave Energy. *Science* **2009**, *323*, 1176–1178.
- (3) Paradiso, J. A.; Starner, T. Energy Scavenging for Mobile and Wireless Electronics. *Pervasive Comput., IEEE* **2005**, *4*, 18–27.
- (4) Donelan, J. M.; Li, Q.; Naing, V.; Hoffer, J. A.; Weber, D. J.; Kuo, A. D. Biomechanical Energy Harvesting: Generating Electricity During Walking with Minimal User Effort. *Science* **2008**, *319*, 807–810.
- (5) Steven, R. A.; Henry, A. S. A Review of Power Harvesting using Piezoelectric Materials (2003–2006). *Smart Mater. Struct.* **2007**, *16*, R1–R21.
- (6) Que, R.; Shao, Q.; Li, Q.; Shao, M.; Cai, S.; Wang, S.; Lee, S.-T. Flexible Nanogenerators Based on Graphene Oxide Films for Acoustic Energy Harvesting. *Angew. Chem., Int. Ed.* **2012**, *51*, 5418–5422.
- (7) Chang, C.; Tran, V. H.; Wang, J.; Fuh, Y.-K.; Lin, L. Direct-Write Piezoelectric Polymeric Nanogenerator with High Energy Conversion Efficiency. *Nano Lett.* **2010**, *10*, 726–731.
- (8) Lee, M.; Chen, C.-Y.; Wang, S.; Cha, S. N.; Park, Y. J.; Kim, J. M.; Chou, L.-J.; Wang, Z. L. A Hybrid Piezoelectric Structure for Wearable Nanogenerators. *Adv. Mater.* **2012**, *24*, 1759–1764.
- (9) Sun, C.; Shi, J.; Bayerl, D. J.; Wang, X. PVDF Microbelts for Harvesting Energy from Respiration. *Energy Environ. Sci.* **2011**, *4*, 4508–4512.
- (10) Heiji, K. The Piezoelectricity of Poly(vinylidene fluoride). *Jpn. J. Appl. Phys.* **1969**, *8*, 975–976.
- (11) Lee, C. S.; Joo, J.; Han, S.; Koh, S. K. Multifunctional Transducer using Poly(vinylidene fluoride) Active Layer and Highly Conducting Poly(3,4-ethylenedioxythiophene) Electrode: Actuator and Generator. *Appl. Phys. Lett.* **2004**, *85*, 1841–1843.
- (12) Guyomar, D.; Sebald, G.; Lefeuvre, E.; Khodayari, A. Toward Heat Energy Harvesting using Pyroelectric Material. *J. Intell. Mater. Syst. Struct.* **2009**, *20*, 265–271.
- (13) Jonathan, G.; Joel, F.; Henry, A. S.; Kevin, F. Energy Harvesting from a Backpack Instrumented with Piezoelectric Shoulder Straps. *Smart Mater. Struct.* **2007**, *16*, 1810–1820.
- (14) Qi, Y.; McAlpine, M. C. Nanotechnology-Enabled Flexible and Biocompatible Energy Harvesting. *Energy Environ. Sci.* **2010**, *3*, 1275–1285.
- (15) Fabretto, M. V.; Evans, D. R.; Mueller, M.; Zuber, K.; Hojati-Talemi, P.; Short, R. D.; Wallace, G. G.; Murphy, P. J. Polymeric Material with Metal-like Conductivity for Next Generation Organic Electronic Devices. *Chem. Mater.* **2012**, *24*, 3998–4003.
- (16) Hojati-Talemi, P.; Bächler, C.; Fabretto, M.; Murphy, P.; Evans, D. Ultrathin Polymer Films for Transparent Electrode Applications

Prepared by Controlled Nucleation. *ACS Appl. Mater. Interfaces* **2013**, *5*, 11654–11660.

(17) Winther-Jensen, B.; Winther-Jensen, O.; Forsyth, M.; MacFarlane, D. R. High Rates of Oxygen Reduction over a Vapor Phase–Polymerized PEDOT Electrode. *Science* **2008**, *321*, 671–674.

(18) Cottis, P. P.; Evans, D.; Fabretto, M.; Pering, S.; Murphy, P.; Hojati-Talemi, P. Metal-Free Oxygen Reduction Electrodes Based on Thin PEDOT Films with High Electrocatalytic Activity. *R. Soc. Chem. Adv.* **2014**, *4*, 9819–9824.

(19) Zhang, W.; Zhao, B.; He, Z.; Zhao, X.; Wang, H.; Yang, S.; Wu, H.; Cao, Y. High-Efficiency ITO-Free Polymer Solar Cells Using Highly Conductive PEDOT:PSS/Surfactant Bilayer Transparent Anodes. *Energy Environ. Sci.* **2013**, *6*, 1956–1964.

(20) Lipomi, D. J.; Bao, Z. Stretchable, Elastic Materials and Devices for Solar Energy Conversion. *Energy Environ. Sci.* **2011**, *4*, 3314–3328.

(21) Pozo-Gonzalo, C.; Mecerreyes, D.; Pomposo, J. A.; Salsamendi, M.; Marcilla, R.; Grande, H.; Vergaz, R.; Barrios, D.; Sánchez-Pena, J. M. All-Plastic Electrochromic Devices based on PEDOT as Switchable Optical Attenuator in the near IR. *Sol. Energy Mater. Sol. Cells* **2008**, *92*, 101–106.

(22) Wu, X.; Li, F.; Wu, W.; Guo, T. Flexible Organic Light Emitting Diodes based on Double-Layered Graphene/PEDOT:PSS Conductive Film formed by Spray-Coating. *Vacuum* **2014**, *101*, 53–56.

(23) Nguyen, P. Q. M.; Yeo, L.-P.; Lok, B.-K.; Lam, Y.-C. Patterned Surface with Controllable Wettability for Inkjet Printing of Flexible Printed Electronics. *ACS Appl. Mater. Interfaces* **2014**, *6*, 4011–4016.

(24) Brooke, R.; Evans, D.; Dienel, M.; Hojati-Talemi, P.; Murphy, P.; Fabretto, M. Inkjet Printing and Vapor Phase Polymerization: Patterned Conductive PEDOT for Electronic Applications. *J. Mater. Chem. C* **2013**, *1*, 3353–3358.

(25) Printz, A. D.; Chan, E.; Liong, C.; Martinez, R. S.; Lipomi, D. J. Photoresist-Free Patterning by Mechanical Abrasion of Water-Soluble Lift-off Resists and Bare Substrates: Toward Green Fabrication of Transparent Electrodes. *PLoS One* **2013**, *8*, Article No. e83939.

(26) Yaghmazadeh, O.; Cicoira, F.; Bernards, D. A.; Yang, S. Y.; Bonnassieux, Y.; Malliaras, G. G. Optimization of Organic Electrochemical Transistors for Sensor Applications. *J. Polym. Sci., Part B: Polym. Phys.* **2011**, *49*, 34–39.

(27) Vosgueritchian, M.; Lipomi, D. J.; Bao, Z. Highly Conductive and Transparent PEDOT:PSS Films with a Fluorosurfactant for Stretchable and Flexible Transparent Electrodes. *Adv. Funct. Mater.* **2012**, *22*, 421–428.

(28) Lipomi, D. J.; Lee, J. A.; Vosgueritchian, M.; Tee, B. C. K.; Bolander, J. A.; Bao, Z. Electronic Properties of Transparent Conductive Films of PEDOT:PSS on Stretchable Substrates. *Chem. Mater.* **2012**, *24*, 373–382.

(29) Savagatrup, S.; Printz, A. D.; O'Connor, T. F.; Zaretski, A. V.; Lipomi, D. J. Molecularly Stretchable Electronics. *Chem. Mater.* **2014**, *26*, 3028–3041.

(30) Noh, J.-S. Highly Conductive and Stretchable Poly-(dimethylsiloxane):Poly(3,4-ethylenedioxythiophene):Poly(styrene sulfonic acid) Blends for Organic Interconnects. *R. Soc. Chem. Adv.* **2014**, *4*, 1857–1863.

(31) Lee, C. S.; Joo, J.; Han, S.; Koh, S. K. An Approach to Durable PVDF Cantilevers with Highly Conducting PEDOT/PSS (DMSO) Electrodes. *Sens. Actuators, A* **2005**, *121*, 373–381.

(32) Schmidt, V. H.; Lediaev, L.; Polasik, J.; Hallenberg, J. Piezoelectric Actuators Employing PVDF Coated with Flexible PEDOT-PSS Polymer Electrodes. *IEEE Trans. Dielectr. Electr. Insul.* **2006**, *13*, 1140–1148.

(33) Polasik, J. T.; Schmidt, V. H. Conductive Polymer PEDOT/PSS Electrodes on the Piezoelectric Polymer PVDF. *Proc. SPIE* **2005**, *5759*, 114–120.

(34) Hojati-Talemi, P.; Evans, D.; Fabretto, M. Extending the Utility of Conducting Polymers through Chemisorption of Nucleophiles. *Chem. Mater.* **2013**, *25*, 1837–1841.

(35) Gelfandbein, V.; Perlman, M. Substrate Effects on Crystallization of Polyvinylidene Fluoride from Solution. *J. Mater. Sci.* **1983**, *18*, 3183–3189.

(36) Ince-Gunduz, B. S.; Alpern, R.; Amare, D.; Crawford, J.; Dolan, B.; Jones, S.; Kobylarz, R.; Reveley, M.; Cebe, P. Impact of Nanosilicates on Poly(vinylidene fluoride) Crystal Polymorphism: Part 1. Melt-Crystallization at High Supercooling. *Polymer* **2010**, *51*, 1485–1493.

(37) Winther-Jensen, B.; Fraser, K.; Ong, C.; Forsyth, M.; MacFarlane, D. R. Conducting Polymer Composite Materials for Hydrogen Generation. *Adv. Mater.* **2010**, *22*, 1727–1730.

(38) Mueller, M.; Fabretto, M.; Evans, D.; Hojati-Talemi, P.; Gruber, C.; Murphy, P. Vacuum Vapour Phase Polymerization of High Conductivity PEDOT: Role of PEG-PPG-PEG, the Origin of Water, and Choice of Oxidant. *Polymer* **2012**, *53*, 2146–2151.

(39) Fabretto, M.; Jariego-Moncunill, C.; Autere, J.-P.; Michelmore, A.; Short, R. D.; Murphy, P. High Conductivity PEDOT Resulting from Glycol/Oxidant Complex and Glycol/Polymer Intercalation during Vacuum Vapour Phase Polymerisation. *Polymer* **2011**, *52*, 1725–1730.

(40) Köster, W.; Franz, H. Poisson's Ratio for Metals and Alloys. *Metall. Rev.* **1961**, *6*, 1–56.

(41) Lee, Y. Y.; Lee, J. H.; Cho, J. Y.; Kim, N. R.; Nam, D. H.; Choi, I. S.; Nam, K. T.; Joo, Y. C. Stretching-Induced Growth of PEDOT-Rich Cores: A New Mechanism for Strain-Dependent Resistivity Change in PEDOT:PSS Films. *Adv. Funct. Mater.* **2013**, *23*, 4020–4027.

(42) Lang, S.; Muensit, S. Review of Some Lesser-Known Applications of Piezoelectric and Pyroelectric Polymers. *Appl. Phys. A: Mater. Sci. Process.* **2006**, *85*, 125–134.

(43) Xie, J.; Mane, X.; Green, C.; Mossi, K.; Leang, K. K. Performance of Thin Piezoelectric Materials for Pyroelectric Energy Harvesting. *J. Intell. Mater. Syst. Struct.* **2010**, *21*, 243–249.

(44) Fabretto, M.; Hall, C.; Vaithianathan, T.; Innis, P.; Mazurkiewicz, J.; Wallace, G.; Murphy, P. The Mechanism of Conductivity Enhancement in Poly(3,4-ethylenedioxythiophene)–Poly(styrenesulfonic) Acid using Linear-Diol Additives: Its Effect on Electrochromic Performance. *Thin Solid Films* **2008**, *516*, 7828–7835.

■ NOTE ADDED AFTER ASAP PUBLICATION

This paper was published on the Web on April 16, 2015. The name and address for Pejman Talemi have been changed, and corrected version was reposted on April 29, 2015.